Identification and molecular characterization of the mammalian α-kleisin RAD21L

Cristina Gutiérrez-Caballero,[1#] Yurema Herrán,[1#] Manuel Sánchez-Martín,[2] José Ángel Suja,[3] José Luis Barbero,[4] Elena Llano[1,5] and Alberto M. Pendás[1*]*

[1]Instituto de Biología Molecular y Celular del Cáncer (CSIC-USAL), Campus Miguel de Unamuno S/N, 37007 Salamanca, Spain. [2]Departamento de Medicina, Campus Miguel de Unamuno S/N, 37007 Salamanca, Spain. [3]Unidad de Biología Celular, Departamento de Biología, Universidad Autónoma de Madrid, 28049 Madrid, Spain. [4]Departamento de Proliferación Celular y Desarrollo, Centro de Investigaciones Biológicas (CSIC), 28040 Madrid, Spain. [5]Departamento de Fisiología, Campus Miguel de Unamuno S/N, 37007 Salamanca, Spain.

[#]These authors contributed equally

[*]Corresponding authors:

Alberto M. Pendás
Instituto de Biología Molecular y Celular del Cáncer (CSIC-USAL),
Campus Miguel de Unamuno, 37007 Salamanca, Spain.
E-MAIL: amp@usal.es
Tel. 34-923 294809; Fax: 34-923 294743

Or

Elena Llano
Departamento de Fisología, Universidad de Salamanca
Campus Miguel de Unamuno, 37007 Salamanca, Spain.
E-MAIL: ellano@usal.es
Tel. 34-923 294809; Fax: 34-923 294743

Running title: Molecular characterization of mammalian RAD21L

Key words: Cohesins, Kleisin, meiosis, mitosis, chromosome segregation, synaptonemal complex.

Abbreviations: CC, cohesin complex; AE, axial element; LE, lateral element; IP, immunoprecipitation; SC, synaptonemal complex; ORF, open reading frame; WB, Western blot.

Abstract

Meiosis is a fundamental process that generates new combinations between maternal and paternal genomes and haploid gametes from diploid progenitors. Many of the meiosis-specific events stem from the behavior of the cohesin complex (CC), a proteinaceous ring structure that entraps sister chromatids until the onset of anaphase. CCs ensure chromosome segregation, participate in DNA repair, regulate gene expression, and also contribute to synaptonemal complex (SC) formation at meiosis by keeping long-range distant DNA interactions through its conserved structure. Studies from yeast to humans have led to the assumption that Scc1/RAD21 is the α-kleisin that closes the tripartite CC that entraps two DNA molecules in mitosis, while its paralogue REC8 is essential for meiosis. Here we describe the identification of RAD21L, a novel mammalian CC subunit with homology to the RAD21/REC8 α-kleisin subfamily, which is expressed in mouse testis. RAD21L interacts with other cohesin subunits such as SMC1α, SMC1ß, SMC3 and with the meiosis-specific STAG3 protein. Thus, our results demonstrate the existence of a new meiotic-specific CC constituted by this α-kleisin and expand the view of REC8 as the only specific meiotic α-kleisin.

During meiosis, two successive rounds of chromosome segregation occur with a single round of replication which leads to the production of haploid gametes from diploid progenitors[1]. This ploidy reduction is achieved by meiosis-specific events such as pairing, synapsis, crossing over between homologs, suppression of sister centromere separation during the meiosis I (reductional division) and separation of sister chromatids in meiosis II (equational division). Sister chromatid cohesion is mediated by a ring-shaped proteinaceous complex named the cohesin complex (CC), which entraps the sister chromatids from its establishment at the S-phase of the cell cycle until its opening at the onset of anaphase[2-5]. The distinct patterns of chromosome dynamics between mitosis and meiosis II (biorientation) and meiosis I (monoritentation) stem in part from a meiosis-specific mechanism of protection of the centromeric cohesion[6,7] and from differences in the composition of the CC between the somatic and the germline lineages.

The mammalian CC is composed of four proteins: two members of the family of structural maintenance of chromosome proteins (SMC1α and SMC3 at mitosis, and SMC1α or SMC1ß and SMC3 at meiosis), one α-kleisin subunit (SCC1/RAD21 at mitosis and/or REC8 at meiosis), and a HEAT repeat domain protein (STAG1 or STAG2 at mitosis, and STAG1, STAG2 or STAG3 at meiosis)[8,9]. This proteinaceous complex is supposed to form a tripartite ring that can be cleaved at the α-kleisin subunit (either RAD21 or REC8) by the action of separase[8]. The activity of this protease plays a crucial function in the metaphase to anaphase transition[9]. In addition to the structural components of the CC, there are several cohesin-interacting proteins that regulate the dynamics of CC such as PDS5 (two paralogues exist in mammals PDS5A and PDS5B), WAPAL, Sororin, the loading factor NIPBL/SCC2, the lysine acetylases ESCO1/ESCO2, and the yeast lysine deacetylase Hos1[10-12].

An important aspect of the cohesins in meiosis, apart from its function in chromosome dynamics, is related to their contribution to the assembly of the SC and eventually, in the generation of the axis-loop structure of meiotic chromosomes which supports synapsis, recombination and segregation[13-15]. The assembly of the axial

element (AE) of the SC after DNA replication is one of the earliest events of meiosis. In mammals, the cohesin subunits RAD21, REC8, SMC3, SMC1α, SMC1ß, and STAG3 and WAPAL decorate the AEs of the SC from its assembly at leptotene to the full synapsed lateral elements (LEs) at pachytene[16-21]. It is not until diakinesis when most of the structural components of the AEs/LEs are partially removed including cohesins[22]. Based on the inability of yeast Rec8 mutants and meiotic-kleisin-deficient *C. elegans* (Rec8, COH-3 and COH-4) to form AEs, it is becoming widely accepted that cohesins play a pivotal role in the AE assembly[23,24]. However, this requirement is not so evident in mammals since it has been observed that REC8-deficient mice are able to assemble AEs in male and female meiocytes[25]. This fact has been attributed to the coexpression of several α-kleisins in mammalian meiocytes, as is the case for *C. elegans*, which would be masking the essential and conserved function of cohesins in AE assembly[24]. In this work we describe the molecular cloning and biochemical characterization of RAD21L, a novel mammalian protein of the CC with homology to the RAD21/REC8 α-kleisin subfamily. This novel α-kleisin interacts with other cohesin subunits such as SMC1α, SMC1ß, SMC3 and with the meiosis-specific STAG3 but not with STAG1/2. The *Rad21l* transcript is detected by Northern blot analysis only in testis. Accordingly, RAD21L protein is expressed in mouse meiocytes localizing to the AEs/LEs of the SC.

Results and Discussion

Based on the existence of paralogues for most of the cohesin subunits in mammals, and given the fact that other species such as *C. elegans* have five different kleisins, we searched for paralogues of the RAD21/REC8 *in silico* using their conserved N-terminal and C-terminal domains (see Methods). A new ORF encoding for a new protein was obtained from mouse and human by RT-PCR (552 and 556 residues respectively, accession numbers HQ603827 and HQ603828) of RNAs from testis and from the MCF7 cell line respectively. Recently, it has been annotated by the Ensemble as *Rad21l1* (BC171911 Gene Bank). Herein, we will use the name RAD21L. The mouse RAD21L protein shows 56% similarity with mouse RAD21 and 35.7% similarity with mouse REC8, and contains the two Pfam domains present in RAD21/REC8 α-kleisins (Fig. 1). In its paralogue RAD21, these domains interact with the head of SMC1α/ß and SMC3, locking the CC (Fig. 2A).

In order to determine the *Rad21l* transcription pattern in mouse, we carried out RT-PCR of RNAs from different mouse tissues. The amplified product, indicative of positive transcription, was obtained in testis, intestine, brain, bone marrow, cerebellum and ovary (Fig. 2B). Given the non-quantitative measurement of this RT-PCR procedure (35 cycles), we undertook a quantitative analysis by a classical Northern blot technique of these positive tissues. The results obtained showed only a transcript of RAD21L in testis (3.5 Kbs approximately), being undetectable in the remaining tissues (Fig. 2C). Since oocytes are not the predominant cell type in whole ovary extracts, we can not rule out that oocyte could also express RAD21L at moderate levels (see below). From these results, we conclude that RAD21L is expressed very weakly in a variety of somatic tissues, being the testis the only organ with a moderate level of transcription. Interestingly, this situation is also mirrored in the pattern of transcription of REC8 (which is widely accepted to be meiosis-specific) in somatic tissues with an unknown function such as in thymus (www.symatlas.org). Taking together our results of the

transcription analysis of RAD21L, we anticipate that this novel α-kleisin could be playing a major reproductive function in the mouse.

Given the absence of cellular models in the male germline that enable studies of gain and loss of function, we first made use of a heterologous system. Human Embryonic Kidney (HEK) 293T cells were transiently transfected with an expression plasmid encoding RAD21L tagged at the N-terminus and subjected to immunoprecipitation (IP). The two prominent bands obtained were identified by mass spectrometry as SMC1α and SMC3 (Fig. 3A). The efficiency and specificity of the immunoprecipitated proteins were comparable using an expression vector of *Rad21*. This interaction was also validated by Western blot (Fig. 3B). Similarly, RAD21L was also able to interact with SMC1ß as well as with SMC1α (Fig. 3C-D). In order to validate the observed interactions using this overexpression model, we confirmed that transfected RAD21L was targeted to the nucleus and bound to chromatin in a way similar to that expected for a cohesin subunit (Fig. 3E-F).

Aside from the structural subunits of the CC, several additional above mentioned regulatory factors such as PDS5 and WAPAL have been demonstrated to play important roles in the dissociation of most cohesins from sister chromatids at the mitotic prophase in the so-called sister chromatid resolution[26,27]. Recently, the region of interaction of STAG1 with RAD21 has been mapped and proposed to be needed for the assembly and function of WAPAL to the CC [28]. Thus, we next sought to examine whether RAD21L is also able to interact with these subunits. For this purpose, we transiently expressed *Rad21l* in HEK 293T cells as well as two novel engineered expressing vectors with deletions at the region of interaction of RAD21 with STAG1[28] and at the corresponding homologous region of RAD21L ($\Delta_{345,365}$*Rad21l* and $\Delta_{372,392}$*Rad21*). We did not observe interaction of RAD21L/$\Delta_{345,365}$RAD21L with STAG1 and/or STAG2 nor with WAPAL, whereas RAD21 was able to interact with these proteins and its negative control ($\Delta_{372,392}$RAD21) was not, further supporting the specificity of our assay (Fig. 4A-C). Owing to the tetrapartite structure of the cohesin core complex and to the expression of RAD21L at testis, we asked whether STAG3

could be the HEAT repeat domain protein that interacts with this new α-kleisin. Interestingly, RAD21L was able to interact with STAG3 (Fig. 5A). This interaction is also observed with RAD21 and is not mediated via the same domain that interacts with STAG1/STAG2. In order to validate these interactions *in vivo*, we carried out IP using antibodies directed against RAD21L in testis extracts. SMC3, SMC1ß and STAG3 but not STAG1 were co-precipitated with RAD21L. Similarly, RAD21L were co-precipitated with SMC1α and SMC3 (Fig. 5B-C). Taken together, we thus conclude that the new α-kleisin RAD21L is able to interact with SMC1α/ß, SMC3 and STAG3 as a new bona fide element of the CC (Fig. 5D) but with distinctive properties such as its inability to interact with STAG1, STAG2 and WAPAL.

We next determined the subcellular localization of RAD21L in meiocytes using two antibodies raised against the C-terminus end of the protein (see Methods for details). To do that, we carried out an analysis of mouse spermatocytes/oocytes spreads using immunofluorescence (IF) colocalization of RAD21L and SYCP3, a structural component of the AEs/LEs that enables meiosis staging. The results showed that RAD21L is located at the AEs and LEs of spermatocytes and oocytes (Fig. 6), similarly to other cohesin subunits such as REC8 and RAD21[17,19]. Thus endogenous RAD21L protein is detected and locates to the SC of both spermatocytes and oocytes.

These conclusions are consistent with two very recent reports (appeared while this manuscript was being edited) using other reagents and strategies[29,30]. In these studies, the same ORF was also identified. The protein, named RAD21L by these two independent groups, is likewise shown to be located at the AEs/LEs of the SC of spermatocytes and oocytes[29,30]. In these works, the pattern of transcription is restricted to reproductive tissues and no transcription was detected in somatic tissues. These discrepancies with our study could be due in part to different sensitivities between the RT-PCR assays. Nevertheless, in both reports, the protein RAD21L is also showed to interact with SMC1α/ß, SMC3 and STAG3 in testis extracts[29,30] which is also the tissue found to express the new protein.

Given that all the cohesin subunits are expressed simultaneously in testis, is very plausible that different CCs could coexist within the same cell at the same time following the tetrapartite ring model: SMC1(α or ß)-SMC3-α-Kleisin(RAD21, REC8 or RAD21L)-STAG(1, 2 or 3) suggesting specific CC program during mammalian meiosis. From our results, we provide experimental evidences showing that RAD21L is able to constitute a meiotic-specific CC with SMC3-SMC1α/ß-STAG3.

Finally, we analysed the genetic relationship of RAD21L with their paralogues RAD21 and REC8 by using an *in silico* analysis of sequenced genomes from sea urchin to humans. This evolutionary analysis shows that RAD21L is most likely a paralogue of RAD21 and is present from bony fish to mammals including reptiles and birds but was lost by the amphibian lineage (Fig. 7). From this analysis, it is interesting to also note the surprising absence of REC8 in the avian lineage, which suggests that RAD21L could have functionally replaced the meiotic function of REC8.

In summary, we provide evidences that RAD21L is a new α-kleisin related with RAD21 which is only expressed at moderate levels in spermatocytes/oocytes. Given the localization of RAD21L at the AEs/LEs of the SC during prophase I and its ability to interact specifically with the meiotic-specific STAG3, we suggest that this α-kleisin participate in the composite molecular processes that are sustained by the SC such as DNA-looping and compaction, pairing, synapsis, and recombination. The functional analysis of a gene-targeted mutation of RAD21L in mouse will undoubtedly shed light on the role that this α-kleisin plays in mammalian gametogenesis.

Acknowledgments

We acknowledge Dr. C. López-Otín for his advice and helpful comments and Dr. V. Quesada for sharing genomic sequence data. We wish to express our sincere thanks to Drs. G.M. Morris, D. Pati, J. Gregan, J.M. Peters and M.B. Kastan for providing antibodies and reagents and I. Ramos-Fernández for technical assistance. This work was supported by SAF, J CyLe (SA) and BFU, and BFU/BCM. C.G.C. and Y.H. are supported by FIS and FPI fellowships respectively. E.L. is recipient of a Ramón y Cajal Research contract.

Methods

Identification and molecular cloning of a novel paralogue of the RAD21/REC8 family of proteins. *In silico* search (tBlastn) with the conserved ~30 residues N-terminal and ~40 residues C-terminal domains of the REC8 and RAD21 proteins against the genome databases of mouse and human, identified two putative exons (corresponding to the ATG and STOP codons) present in most mammals, separated apart in the mouse by 23 Kbs of genomic sequence. *Rad21l* ORF was PCR amplified from cDNA obtained from mouse testis using the following primers S1 5'-ATGTTCTACACTCATGTGCTTATG-3' and AS1 5'- TCACATCTTATAGAACA TTGGTCCC-3'. The human *Rad21l* ORF was reverse amplified from RNA extracted from the MCF7 cell line using the S2 5'- CAGGCAACATGTTCTACACACATGT-3' and AS2 5'-CAGAAATTCCAGTGATGCCATAAAT-3' primers. The human and murine ORFs encode for proteins of 552 and 556 (residues respectively Accession numbers HQ603827 and HQ603828) which have been recently annotated by the Ensemble and named *Rad21l* (BC171911). The gene is composed of 13 exons and spans over 26 and 23 kbs in human and mouse genomes respectively and is located in a syntenic chromosomal segment at 20p13 and 2G3.

Generation of plasmids. Full-length cDNAs encoding *Rad21l*, *Rad21* and *Wapal* were RT-PCR amplified from murine testis RNA. *Smc1β* and *Stag1* cDNAs were obtained from an IMAGE cDNA clone. Full-length cDNAs were cloned into the pcDNA3, pcDNA3 x2Flag, pCEFL HA or pcDNA3.1 Myc-His (-) mammalian expression vectors. The *Rad21l* and *Rad21* mutants ($\Delta_{345,365}$*Rad21l* and $\Delta_{372,392}$*Rad21*) with a deletion at the region that interacts with STAG1, were generated by directed mutagenesis. The pRevTRE 9Myc-*Rad21*, Myc-*Smc1α* and Flag-*Stag2* expression plasmids were kindly provided by Dr. J. Gregan (Max F**.** Perutz Laboratories**,** University of Vienna), Dr. M. B. Kastan (St. Jude Children's Research Hospital, Memphis) and Dr. D. Pati **(**Texas Children's Hospital), respectively.

Antibody production. We have generated two different Abs in the same species (rabbit) using two different antigens. Rabbit *α*RAD21L-AP was raised against a peptide

of RAD21L –CNSHSELDQPQDWKD. Rabbit *α*RAD21L-ARP was raised against a recombinant protein expressed in *E. coli* corresponding to residues 344 to 552 (located at the C-terminus end). IgGs were purified using the Amersham IgG purification Kit. The specificity of both Abs was tested against mouse RAD21 and REC8. For this purpose, we carried out immunofluorescence and Western Blotting using Human Embryonic Kidney (HEK) 293T cells transfected with a plasmid expressing REC8, RAD21 and RAD21L. Cells were fixed similarly to the spermatocytes to mimic the conditions of spermatocyte spreads. Both antibodies showed to specifically recognize RAD21L and did not cross-react neither with RAD21 or REC8. Both RAD21 and REC8 were detected simultaneously with an epitope tagged at either N- or C-terminus to validate that they were successfully transfected and expressed. Both antibodies were used to validate the results of the IF and IP data presented throughout this work.

Immunoprecipitation and antibodies. HEK 293T cells were transiently transfected and whole cell and nuclear extracts were prepared and cleared with protein G Sepharose beads (GE Healthcaere) for 1h. Antibody was added for 2 h. and immunocomplexes were isolated by adsorption to protein G Sepharose beads for 1 hour. After washing, beads were loaded on reducing 8% polyacrylamide SDS gels and proteins were detected by western blotting with the indicated antibodies or silver staining followed by mass spectrometry of the excised and digested bands of interest. Coimmunoprecipitation of WAPAL with cohesins was analyzed using ditiobis succinyl propionate (DSP, 1mg/ml 10´ at 37 ºC) to stabilize their labile protein complexes [31]. Immunoprecipitation of the endogenous protein was performed using whole extracts of testis as previously described[32] but with the addition of 5 mM ß-mercaptoethanol. Immunoprecipitations were performed using rabbit *α*RAD21L AP IgG (1:500), rabbit *α*RAD21L ARP IgG (1:500), mouse αFlag IgG (5µg; F1804, Sigma-Aldrich), rabbit αMyc Tag IgG (4µg; #06-549, Millipore), rabbit αRAD21 IgG K854[33] (1:500), rabbit αSMC1α serum K988[34] (1:250), rabbit αSMC3 serum K987[35](1:250), mouse αHA.11 IgG MMS- (5µL, aprox. 10µg/1mg prot; 101R, Covance), ChromPure mouse IgG 015-000-003 (5µg), ChomPure rabbit IgG (5µg/1mg prot.; 011-000-003, Jackson ImmunoResearch), rabbit αSMC3 agarose immobilized S300-060 (4µg/1mg prot.), and

rabbit αSMC1α agarose immobilized (5μg/1mg prot., S300-055, Bethyl). Primary antibodies used for Western blotting were mouse αFlag IgG (F1804, Sigma-Aldrich) (1:10.000), rabbit αHA IgG (H6908, Sigma-Aldrich) (1:1.000), rabbit αFlag IgG (1:800; F7425 Sigma-Aldrich), mouse αMyc obtained from hybridoma cell myc-1-9E10.2 ATCC (1:5), rabbit αRAD21 serum K854[33] (1:10.000), rabbit αRAD21L serum (1:8.000), rabbit αSMC1α serum K988[34] (1:8.000), rabbit αSMC3 serum K987[35] (1:8.000). Secondary horseradish peroxidase-conjugated α-mouse NA931V (GE Healthcare) or α-rabbit #7074 (Cell Signaling) antibodies were used at 1:10.000 and 1:2.000 dilution, respectively. Antibodies were detected by using Immobilon™ Western Chemiluminescent HRP Substrate from Millipore.

Chromatin fractionation. HEK 293T cells were transfected with Flag-*Rad21l*. Chromatin fractionation was performed as previously described[36]. Thereafter, proteins of nuclear-soluble fraction and chromatin-bound fraction were separated by SDS-PAGE and immunoblotted with mouse αFlag IgG (1:10.000; F1804 Sigma-Aldrich) or mouse αLamin A/C (Manlac-1) (1:100, provided by Dr. G. Morris, Oswestry, UK).

Transcription analysis of *Rad21l* in several tissues. In the absence of ESTs from mouse and very few from humans, we analyzed the transcription by RT-PCR using 5 μg of RNA from kidney, liver, lung, muscle, bone marrow, cerebellum, brain, thymus, uterus, intestine, ovary, spleen, heart and testis, and reverse-transcribed into cDNA using oligo dT. PCR was performed using primers S2 5'-TGGCTTGCAGCTCACTGGGA-3' and AS2 5'-GGTTCTGAGCAAGGGGCTCCG-3' (amplicon´ size 352 bp) (located at exons 1 and 4 respectively). As control, β-actin was also amplified (5´-GCTCCGGCATGTGCAA-3', 5´-AGGATCTTCATG AGGTAGT-3'). 40 μg of total RNA was electrophoresed under denaturing conditions, blotted to Genescreen Plus membrane (Perkin Elmer), and hybridized with the ORF of RAD21L labelled by random priming with dCTP[32] .

MALDI-TOF mass spectrometry analysis. Bands of interest were manually excised and in-gel digested with trypsin. Tryptic peptides were analyzed on a Bruker Ultraflex MALDI-TOF mass spectrometer and searched against NCBI database. Mowse scores with a value greater than 66 were considered as significant ($p<0.05$). The Proteomics Laboratory at IBMCC is a member of ProteoRed funded by Genoma España.

Immunocytology. Testes were detunicated and processed for spreading using a "dry-down" technique[37]. Oocytes from foetal ovaries (E17.5 embryos) were digested with collagenase, incubated in hypotonic buffer, disaggregated, fixed in paraformaldehyde and incubated with the indicated antibodies for immunofluorescence. Primary antibodies used for immunofluorescence were rabbit αRAD21L AP IgG (1:5), rabbit α-RAD21L ARP IgG (1:5) and mouse αSYCP3 IgG (Santa Cruz, sc-74569) (1:100), rabbit αRAD21 serum K854[33] (1:10.000), rabbit αSMC1α serum K988[34] (1:8.000), rabbit αSMC3 serum K987[35] (1:8.000). Secondary antibodies used were TRITC α-mouse (115-095-146)/α-rabbit (111-025-144), FITC- α-mouse (115-095-146)/α-rabbit (111-095-045) (Jackson ImmunoResearch).

Phylogenetic analysis. *Rad21l* orthologs were identified by BLASTP searches of Genbank and other genome webs such as Ensemble. The selected orthologs can be found in Table I. Amino acid alignments were done with ClustalW, using the default settings. The phylogram tree was constructed by using the neighbor-joining method with Poisson correction. The reliability of internal branches was assessed by using 1000 bootstrap with the computer program MEGA4.

REFERENCES

1. Nasmyth K. Segregating sister genomes: the molecular biology of chromosome separation. Science 2002; 297:559-65.

2. Unal E, Heidinger-Pauli JM, and Koshland D. DNA double-strand breaks trigger genome-wide sister chromatid cohesion through Eco1 (Ctf7). Science 2007; 317:245-8.

3. Zhang N, Kuznetsov SG, Sharan SK, Li K, Rao PH, Pati D. A handcuff model for the cohesin complex. J Cell Biol 2008; 183:1019-31.

4. Gruber S, Haering CH, Nasmyth K.Chromosomal cohesin forms a ring. Cell 2003; 112:765-77.

5. Haering CH, Farcas AM, Arumugam P, Metson J, Nasmyth K. The cohesin ring concatenates sister DNA molecules. Nature 2008; 454:297-301.

6. Kitajima TS, Sakuno T,Ishiguro, K,Iemura S, Natsume T,. Kawashima SA., Watanabe Y. Shugoshin collaborates with protein phosphatase 2A to protect cohesin. Nature 2006; 441:46–52.

7. Llano E, Gómez R, Gutiérrez-Caballero C, Herrán Y, Sánchez-Martín M, Vázquez-Quiñones L, Hernández T, de Alava E, Cuadrado A, Barbero JL, Suja JA, Pendás AM. Shugoshin-2 is essential for the completion of meiosis but not for mitotic cell division in mice. Genes Dev. 2008; 22:2400-13.

8. Watanabe, Y. Sister chromatid cohesion along arms and at centromeres. Trends Genet 2005; 21:405–12.

9. Hirano, T. At the heart of the chromosome: SMC proteins in action. Nat Rev Mol Cell Biol 2006; 7:311–22.

10. Nishiyama T, Ladurner R, Schmitz J, Kreidl E, Schleiffer A, Bhaskara V, Bando M, Shirahige K, Hyman AA, Mechtler K, Peters JM. Sororin mediates sister chromatid cohesion by antagonizing Wapl. Cell 2010 ;143:737-49.

11. Borges V, Lehane C, Lopez-Serra L, Flynn H, Skehel M, Rolef Ben-Shahar T, Uhlmann F. Hos1 deacetylates Smc3 to close the cohesin acetylation cycle. Mol Cell 2010;39:677-88.

12. Nasmyth K, Haering CH. Cohesin: its roles and mechanisms. Annu Rev Genet 2009; 43:525-58.

13. Page SL, Hawley RS. The genetics and molecular biology of the synaptonemal complex. Annu Rev Cell Dev Biol 2004;20:525-58.

14. Revenkova E, Jessberger R. Shaping meiotic prophase chromosomes: cohesins and synaptonemal complex proteins. Chromosoma 2006; 115:235-40.

15. Yang F, Wang PJ. The Mammalian synaptonemal complex: a scaffold and beyond. Genome Dyn 2009; 5:69-80.

16. Parra MT, Viera A, Gómez R, Page J, Benavente R, Santos JL, Rufas JS, Suja JA. Involvement of the cohesin Rad21 and SCP3 in monopolar attachment of sister kinetochores during mouse meiosis I. J Cell Sci 2004; 117:1221-34.

17. Eijpe M, Heyting C, Gross B, Jessberger R. Association of mammalian SMC1 and SMC3 proteins with meiotic chromosomes and synaptonemal complexes. J Cell Sci 2000; 113:673-82.

18. Revenkova E, Eijpe M, Heyting C, Gross B, Jessberger R. Novel meiosis-specific isoform of mammalian SMC1. Mol Cell Biol 2001; 21:6984-98.

19. Prieto I, Suja JA, Pezzi N, Kremer L, Martínez-A C, Rufas JS, Barbero JL. Mammalian STAG3 is a cohesin specific to sister chromatid arms in meiosis I. Nat Cell Biol 2001; 3:761-6.

20. Zhang J, Håkansson H, Kuroda M, Yuan L. Wapl localization on the synaptonemal complex, a meiosis-specific proteinaceous structure that binds homologous chromosomes, in the female mouse. Reprod Domest Anim 2008; 43:124-6.

21. Pelttari J, Hoja MR, Yuan L, Liu JG, Brundell E, Moens P, Santucci-Darmanin S, Jessberger R, Barbero JL, Heyting C, Höög C. A meiotic chromosomal core consisting of cohesin complex proteins recruits DNA recombination proteins and promotes synapsis in the absence of an axial element in mammalian meiotic cells. Mol Cell Biol 2001; 21:5667-77.

22. Suja JA, Barbero JL. Cohesin complexes and sister chromatid cohesion in mammalian meiosis. Genome Dyn 2009; 5:94-116.

23. Klein F, Mahr P, Galova M, Buonomo SB, Michaelis C, Nairz K, Nasmyth K. A central role for cohesins in sister chromatid cohesion, formation of axial elements, and recombination during yeast meiosis. Cell 1999; 98: 91-103.

24. Severson AF, Ling L, van Zuylen V, Meyer BJ. The axial element protein HTP-3 promotes cohesin loading and meiotic axis assembly in C. elegans to implement the meiotic program of chromosome segregation. Genes Dev 2009; 23:1763-78.

25. Xu H, Beasley MD, Warren WD, van der Horst GT, McKay MJ. Absence of mouse REC8 cohesin promotes synapsis of sister chromatids in meiosis. Dev Cell 2005; 8:949–61.

26. Kueng S, Hegemann B, Peters BH, Lipp JJ, Schleiffer A, Mechtler K, Peters JM. Wapl controls the dynamic association of cohesin with chromatin. Cell 2006; 127:955-67.

27. Losada A, Yokochi T, Hirano T. Functional contribution of Pds5 to cohesin-mediated cohesion in human cells and Xenopus egg extracts. J Cell Sci 2005;118:422-33.

28. Shintomi K, Hirano T. Releasing cohesin from chromosome arms in early mitosis: opposing actions of Wapl-Pds5 and Sgo1. Genes Dev 2009; 23:2224-36.

29. Lee J, Hirano T. RAD21L, a novel cohesin subunit implicated in linking homologous chromosomes in mammalian meiosis. J Cell Biol 2011; 192:263-76.

30. Ishiguro K, Kim J, Fujiyama-Nakamura S, Kato S, Watanabe Y. A new meiosis-specific cohesin complex implicated in the cohesin code for homologous pairing. EMBO Rep 2011;12:267-75.

31. Terret ME, Sherwood R, Rahman S, Qin J, Jallepalli PV. Cohesin acetylation speeds the replication fork. Nature 2009; 462:231-34.

32. Kolli S, Zito CI, Mossink MH, Wiemer EA, Bennett AM. The major vault protein is a novel substrate for the tyrosine phosphatase SHP-2 and scaffold protein in epidermal growth factor signaling.J Biol Chem 2004; 279:29374-85.

33. Prieto I, Pezzi N, Buesa JM, Kremer L, Barthelemy I, Carreiro C, Roncal F, Martinez A Gomez L, Fernandez R, et al. STAG2 and Rad21 mammalian mitotic cohesins are implicated in meiosis EMBO rep 2002; 3:543–50.

34. Krasikova A, Barbero JL, Gaginskaya E. Cohesion proteins are present in centromere protein bodies associated with avian lampbrush chromosomes. Chromosome Res 2005; 13:675-68.

35. Prieto I, Tease C, Pezzi N, Buesa JM, Ortega S, Kremer L, Martínez A, Martínez-A C, Hultén MA, Barbero JL. Cohesin component dynamics during meiotic prophase I in mammalian oocytes. Chromosome Res 2004; 12:197–213.

36. Santos MA, Huen MS, Jankovic M, Chen HT, López-Contreras AJ, Klein IA, Wong N, Barbancho JL, Fernandez-Capetillo O, Nussenzweig MC, et al. Class switching and meiotic defects in mice lacking the E3 ubiquitin ligase RNF8. J Exp Med 2010; 207:973-81.

37. Peters AH, Plug AW, van Vugt MJ, de Boer P.. Drying-down technique for the spreading of mammalian meiocytes from the male and female germline. Chromosome Res 1997; 5:66-71.

Table 1

			Protein-Gene Identification		
Species	**Group**	**Abrev.**	**Rad21L**	**Rad21**	**Rec8**
Homo sapiens	Hominid	Hs	+/this work HQ603827	+/ O60216	+/ Q8C5S7
Mus musculus	Rodent	Mm	+/this workHQ603828	+/ Q61550	+/ O95072
Sus scrofa	Laurasiatheria	Ss	+/ENSSSCP00000007658	+/ENSSSCP00000006424	+/ ENSSSCP00000002187
Monodelphis domestica	Marsupial	Md	+/ENSMODP00000024381	pp/chr3:389108458-389129090	+/ENSMODP00000034072
Gallus gallus	Birds	Gg	+/ENSGALG00000006186	+/Q5ZLK3	----------
Taeniopygia guttata	Birds	Tg	+/ ENSTGUP00000007091	+/ENSTGUP00000012686	----------
Meleagris gallopavo	Birds	Mg	+/ENSMGAP00000008199	+/ENSMGAP00000013148	----------
Anolis carolinensis	Reptile	Ac	P/ENSACAP00000008231	+/ENSACAP00000010827	P/ENSACAP00000003857
Xenopus tropicalis	Amphibia	Xt	----------	+/ENSXETP00000044903	+/ ENSXETG00000014620
Danio rerio	Fish	Dr	+/ ENSDARP00000074083	+/Q7ZW30	+/ENSDARP00000091417 +/ENSDARP00000091005
Oryzias latipes	Fish	Ol	+/ENSORLP00000018323	+/ ENSORLG00000005535	pp
Takifugu rubripes	Fish	Tr	+/ENSTRUP00000007429	+/ENSTRUP00000017209	pp
Ciona intestinalis	Tunicate	Ci	----------	+/ENSCINP00000022121	p/ENSCINP00000021677
Ciona savignyi	Tunicate	Cs	----------	p/ENSCSAVP00000001613	p/ ENSCSAVG00000004732
Strongylocentrotus purpuratus	Echinoderm	Sp	----------	+/xp_001176016	+/XP_001200458

The presence of genomic sequences coding for full protein is indicated with a "+". When most of the full protein is present in the translated genomic sequence is indicated with a "p", whereas the existence of only genomic sequences coding for part of the protein is denoted with "pp" and were not used in the alignment but only as a first hint of its likely existence in that species.------ indicates the absence of the protein in the genome.

Legend to figures

Figure 1. Alignment of the three members of the α-kleisin family (RAD21L, RAD21 and REC8) from mouse (Mm) and human (Hs). The mouse and human ORFs of RAD21L, RAD21 and REC8 were translated and the proteins aligned using CLUSTAL. The mouse RAD21L protein has 56% similarity (41% identity) with mouse RAD21 and 35.7% similarity (21% identity) with mouse REC8 and contains the two Pfam domains present in RAD21/REC8 α-kleisins; the so-called "RAD21/REC8 N-terminus domain" (expanding from residues 1 to 111) and a C-terminus domain named "Conserved region of RAD21/REC8 like proteins" (expanding from residues 496-548 in the mouse). These domains are underlined. The regions deleted in the mutant mouse proteins $\Delta_{345,365}$RAD21L and $\Delta_{372,392}$RAD21 are bolded and underlined in the corresponding sequence.

Figure 2. Model of the cohesin complex and mouse tissue expression pattern of *Rad21l*. (A) Schematic representation of the ring-like model of the mammalian CC and the cohesin-regulator WAPAL. In the ring model of the CC two members of the SMC family (SMC1α/ß and SMC3) associate with one α-kleisin subunit that closes the ring (RAD21 or REC8) and with a HEAT repeat domain protein (STAG1, STAG2, or STAG3). (B) RT-PCR of RNAs from the indicated mouse tissues was analyzed by agarose gel electrophoresis using primers S2 and AS2 to amplify a 352 bp fragment of *Rad21l*. RT-PCR of a fragment of the ß-Actin RNA was used as control. (C) Tissue expression of murine *Rad21l* by Northern blot.

Figure 3. Biochemical characterization of RAD21L and nuclear localization of the overexpressed protein. HEK 293T cells were transfected or cotransfected with the indicated expression vectors or empty vector. IP was performed with the indicated antibody. Input (20 μg) and IP samples were resolved by SDS-PAGE and silver stained (SILVER) or Western-blotted (WB) with the indicated antibody. Immunoprecipitation of Flag-RAD21/Myc-RAD21 was used in all the experiments as positive control. (A) The two endogenous proteins that immunoprecipitate with Flag-RAD21L and Flag-RAD21 (positive control) were analyzed by mass spectrometry showing to be SMC1α and SMC3. The same immunoprecipitates were immunoblotted with anti-SMC1α and anti-SMC3 (B). (C) RAD21L immunoprecipitates with Flag-SMC1β. (D) RAD21L interacts with either SMC1α or SMC1β. Cells were cotransfected with *Rad21l* together with Myc-*Smc1α* and/or Flag-*Smc1β*. IP was performed with anti-RAD21L, anti-Myc or anti-Flag and was analyzed by immunoblotting with the indicated antibody. (E) Nuclear localization of RAD21L. IF detection of transfected RAD21L in HEK 293T cells with an antibody against RAD21L. Nuclei were counterstained with DAPI. (F) Transfected RAD21L is found in the chromatin-bound fraction. HEK 293T cells were transfected with Flag-*Rad21l* and chromatin was isolated and digested with micrococcal nuclease to release chromatin-bound proteins. Both nuclear-soluble fraction (*soluble*) and chromatin-bound fraction (*chromatin*) were resolved by SDS-PAGE and blotted with anti-Flag. Antibody against Lamin A/C was used as positive control of the soluble fraction. EV: Empty vector. IP: Immunoprecipitation. WB: Western Blot. R21: α-RAD21. L: α-RAD21L. IgG: negative control with whole rabbit or mouse IgG.

Figure 4. STAG1, STAG2 and WAPAL do not interact with RAD21L. HEK 293T cells were transfected or cotransfected with the indicated expression vectors or empty vector. IP was performed with the indicated antibody. IP samples were resolved by SDS-PAGE and Western-blotted with the indicated antibody. Immunoprecipitation of Flag-$\Delta_{372,392}$RAD21 was used as negative control in the co-immunoprecipitation with STAG1 and STAG2. Flag-RAD21L does not immunoprecipitate HA-STAG1 (A), Flag-STAG2 (B) and Flag-WAPAL (C). EV: Empty vector. IP: Immunoprecipitation. WB: Western Blot. R21: α-RAD21. L: α-RAD21L. IgG: negative control with whole rabbit or mouse IgG. Rad21Δ: $\Delta_{372,392}$ RAD21. Rad21lΔ: $\Delta_{345,365}$ RAD21L.

Figure 5. Analysis of the interactions of the subunits of the cohesin complex with RAD21L and proposed model of the new cohesin complex. (A) Flag-RAD21L and Flag-RAD21 immunoprecipitate Myc-STAG3 and the IP is not disturbed by the deletion of the interacting region in RAD21 (RAD21Δ) or in its counterpart region in RAD21L (RAD21LΔ). (B-C) Whole testis extracts were immunoprecipitated with the corresponding antibody. (B) Endogenous RAD21L interacts with SMC proteins. (C) RAD21L immunoprecipitates SMC proteins and STAG3 but not STAG1. (D) Proposed model of the CC following the most accepted ring configuration in which RAD21L would interact with SMC1 and SMC3 and with the STAG3 subunit but not with WAPAL. EV: Empty vector. IP: Immunoprecipitation. WB: Western Blot. R21: α-

RAD21. L: α-RAD21L. IgG: negative control with whole rabbit or mouse IgG. Rad21Δ: $\Delta_{372,392}$ RAD21. Rad21lΔ: $\Delta_{345,365}$ RAD21L.

Figure 6. RAD21L is located at the LEs of the SC of mouse meiocytes. (A) Double immunolabeling of RAD21L (green) and SYCP3 (red) in a wild-type spermatocyte at early pachytene. (B) Double immunolabeling of RAD21L and SYCP3 in a pachytene oocyte.

Figure 7. Phylogenetic tree of presumed RAD21L, RAD21 and REC8 orthologs. The database sequence accession number of each protein is presented in Table I. The indicated numbers represent the bootstrap values. Major phylogenetic groups are indicated.

Fig. 1


Hs_Rad21L MFYTHVLMSKRGPLAKIWLAAHWEKKLTKAHVFECNLEITIEKILS----------PKVKIALRTSGHLLLGVVRIYNRKAKYLLADCSEAFLKMKMTFRPGLVDLPKENFEASYN 106
Mm_Rad21L MFYTHVLMSKRGPLAKIWLAAHWEKKLTKAHVFECNLEITIQKIIS----------PKVKIALRTSGHLLLGVVRIYNRKAKYLLADCSEAFLKMKMTFRPGLVDLPKENFEAAYN 106
Mm_Rad21 MFYAHFVLSKRGPLAKIWLAAHWDKKLTKAHVFECNLESSVESIIS----------PKVKMALRTSGHLLLGVVRIYHRKAKYLLADCNEAFIKIKMAFRPGVVDLPEENREAAYN 106
HS_Rad21 MFYAHFVLSKRGPLAKIWLAAHWDKKLTKAHVFECNLESSVESIIS----------PKVKMALRTSGHLLLGVVRIYHRKAKYLLADCNEAFIKIKMAFRPGVVDLPEENREAAYN 106
Mm_Rec8 MFYYPNVLQRHTGCFATIWLAATRGSRLVKREYLNVNVVKTCEEILNYVLVRVQPPVAGLPRPRFSLYLSAQLQIGVIRVYFQQCQYLVEDIQHILEHLHRAQLRIRIDMEEADLPSLLL 120
HS_Rec8 MFYYPNVLQRHTGCFATIWLAATRGSRLVKREYLRVNVVKTCEEILNYVLVRVQPPQPGLPRPRFSLYLSAQLQIGVIRVYSQQCQYLVEDIQHILERLHRAQLQIRIDMET-ELPSLLL 119
RAD21/REC8 N-terminus domain
Hs_Rad21L --AITLPEEFHDFDT--QNMNAIDVSEHFTQNQSRPEEITLRENFDNDLLFQAESFG----EESEILRRHSFFDDN-ILLNSSG----PLIEHSSGSLTGER-SLFYD---SGDGFGDEG 209
Mm_Rad21L --TITLPEEFHDFEI--YNINEIDISEPLAQNQSRPEEITLREEYSNDLLFQAGSFG----DEPEILRRHSFFDDN-ILMNSSG----LVVEHSSGSFAEEK-SLFFD---NGDGFGDEG 209
Mm_Rad21 --AITLPEEFHDFDQPLPDLDDIDVAQQFSLNQSRVEEITMREEVGNISILQENDFGDFGMDDREIMREGSAFEDDDMLVSTSASNLLLEPEQSTSNLNEKMNHLEYEDQYKDDNFGEGN 224
HS_Rad21 --AITLPEEFHDFDQPLPDLDDIDVAQQFSLNQSRVEEITMREEVGNISILQENDFGDFGMDDREIMREGSAFEDDDMLVSTTTSNLLLESEQSTSNLNEKINHLEYEDQYKDDNFGEGN 224
Mm_Rec8 PNCLAMMETLEDAPEPFFGKMSVDPRLPSPFDIPQIRHLLEAATPEKTRKETLPEATPDPRKPDRTLATVQSPEVITLQEAEPIRMLQIEGEQDLPEISRGDLELLIAEKDDAILLEERQ 240
HS_Rec8 PNHLAMMETLEDAPDPFFGMMSVDPRLPSPFDIPQIRHLLEAAIPER-VEEIPPEVPTEPREPERIPVTVLPPEAITILEAEPIRMLEIEGERELPEVSRRELDLLIAEEEEAILLEIPR 238
--→
Hs_Rad21L AAGEMIDNLLQDDQNILLED--MHLNREISLPSEPPNSLAVEPDN----------SECICVPENEKMNETILLSTEEEGFTLDP------IDISDIAEKRKGKKRRLLIDPIKELSSKVI 311
Mm_Rad21L AAGEMIDNLLQDE-STFLEE--AYLNKEVSLPPELPSSIMVEPGN----------SDDQCIPEDEEINEITLLSNEDEGFTLDP------IDDLDIADRRRRKKRRLLVDPVKEISSKAM 310
Mm_Rad21 DGGILDDKLISNNDGGIFDDPPALSEAGVMLPEQPAHDDMDEDDNGSLGGPDSPDSVDPVEPMPTMTDQTTLVPNEEEAFALEP------IDIT-VKETKAKRKRKLIVDSVKELDSKTI 337
HS_Rad21 DGGILDDKLISNNDGGIFDDPPALSEAGVMLPEQPAHDDMDEDDNVSMGGPDSPDSVDPVEPMPTMTDQTTLVPNEEEAFALEP------IDIT-VKETKAKRKRKLIVDSVKELDSKTI 337
Mm_Rec8 RGRLLRQRRASLPLDESREEPRALEGAGLVSALSPPAPAQVEGIQEALPGQVFPPEVQKMTGWEPGALLTEVTPPQELRLPAPPSTEKRLPSLQRPLPRRHRRRQLLFWDKETQISREKF 360
HS_Rec8 --------------------------------LPPPAPAEVEGIGEALG-----PEELRLTGWEPGALLMEVTPPEELRLPAPPSPERRPP--VPPPPRRRRRRRLLFWDKETQISPEKF 319
Hs_Rad21L HKQLTSFADTLMVLELAPPTQRLMMWKKRGGVHTLLSTAAQDLIHAELKMLFTKCF---LSSGFKLGR--------KMIQKESVREEVGNQ------------NIVETSMMQEPN---- 403
Mm_Rad21L HRQLASFMDTLMVLDLAPPTQRLMMWKKRGGVDMLLSTATQDLINDELKMLFTKCF---LSSDYKLA---------KLTLKESVRKEVGNQ------------QIAEPSVMGEPN---- 401
Mm_Rad21 RAQLSDYSDIVTTLDLAPPTKKLMMWKETGGVEKLFSLPAQPLWNNRLLKLFTRCLTPLVPEDLRKRRKGGEADNLDEFLKEFENPEVPREEQQPQQQQPQPQRDVIDEPIIEEPSRLQD 457
HS_Rad21 RAQLSDYSDIVTTLDLAPPTKKLMMWKETGGVEKLFSLPAQPLWNNRLLKLFTRCLTPLVPEDLRKRRKGGEADNLDEFLKEFENPEVPREDQQQQHQQ----RDVIDEPIIEEPSRLQE 453
Mm_Rec8 EEQLQTGAHCWEYPVAQPPKR-----MLTSPAELFRTPTLSGWLPPELLGLWTHCAQ--VPQRMLRQRP-------QLETEETVEEERAAD--------------EEERRKTEALS---- 448
HS_Rec8 QEQLQTRAHCWECPMVQPPER-----TIRGPAELFRTPTLSGWLPPELLGLWTHCAQ--PPPKALRR---------ELP-------EEAAA--------------EEERRKIEVPS---- 398
Hs_Rad21L -----YQQELSK----PQTWKDVIGGSQHSSHEDTNKNINSEQDIVEMVSLAAEESSLMNDLFAQEIEYSPVELE---------------SLSNEENIETERWNGRILQMLN-RLRESNK 498
Mm_Rad21L -----SHSELDQ----PQDWKDVTDESVGSFQENVNMNVNSEQDILGMISPAVEGLSSMNGSLAQEN--CPAELE---------------SSGSKQNTEAEKWNQRLFQTLN-VLREFNK 494
Mm_Rad21 SVMEASRTTIEESAMPPPPPQGVKRKAGQIDPEPSIPPQQVEQMEIPPVELPPEEPPNICQLIPELELLPEKEKEKEKEKEEEEEEEDEDASGGDQDQEERRWNKRTQQMLHGLQRALAK 577
HS_Rad21 SVMEASRTNIDESAMPPPPPQGVKRKAGQIDPEPVMPPQQVEQMEIPPVELPPEEPPNICQLIPELELLPEKEKEKEKEKEDDEEEEDEDASGGDQDQEERRWNKRTQQMLHGLQRALAK 573
Mm_Rec8 ------EIEVLREAQEPSGPLMLSSELSLEAAEDEKSRTSLIPP-EWWAWSEEGQPEPPALPMLPELPEVPMEMP--------------------PRPE-----LSSEAVLRAVALKLQA 536
HS_Rec8 ------EIEVPREALEPSVPLMVSLEISLEAAEEEKSRISLIPPEERWAWPEVEAPEAPALPVVPELPEVPMEMP--------------------LVLPPELELLSLEAVHRAVALELQA 492
Hs_Rad21L MGMQSFSLMKLCRNSDRKQAAAKFYSFLVLKKQLAIELSQSAPYADIIATMGPMFYNI 556
Mm_Rad21L MGMQSFSLKKLCRNSDRKQAAAKFYTLLILKKHRAIELSQSVPYADIIATVGPMFYKM 552
Mm_Rad21 TGAESISLLELCRNTNRKQAAAKFYSFLVLKKQQAIELTQEEPYSDIIATPGPRFHII 635
HS_Rad21 TGAESISLLELCRNTNRKQAAAKFYSFLVLKKQQAIELTQEEPYSDIIATPGPRFHII 631
Mm_Rec8 NKELDFSSLVPPLSP-RKLASRVFYLLLVLSTQKILLVEQQKPYGPLLIRPGPKFP- 591
HS_Rec8 NREPDFSSLVSPLSP-RRMAARVFYLLLVLSAQQILHVKQEKPYGRLLIQPGPRFH-- 547
←----------→
Conserved region of Rad21/Rec8 like protein

A

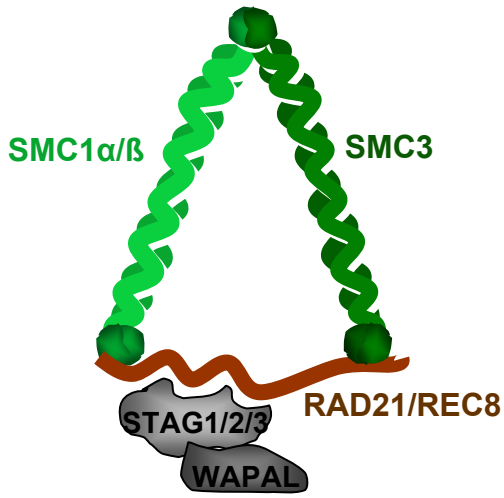
SMC1α/ß
SMC3
RAD21/REC8
STAG1/2/3
WAPAL

B

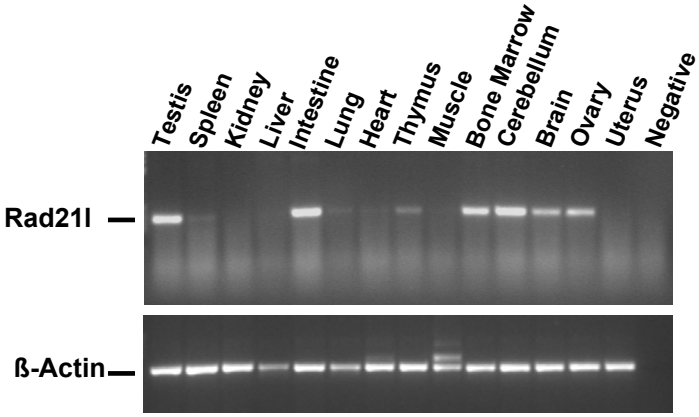
Testis
Spleen
Kidney
Liver
Intestine
Lung
Heart
Thymus
Muscle
Bone Marrow
Cerebellum
Brain
Ovary
Uterus
Negative
Rad21l
ß-Actin

C

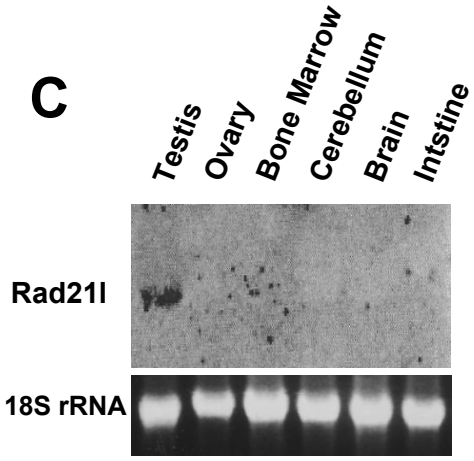
Testis
Ovary
Bone Marrow
Cerebellum
Brain
Intstine
Rad21l
18S rRNA

A

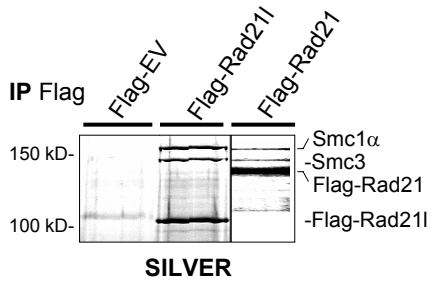

Protein	Score	Peptide number	Sequence Cover
Smc1α	284	35	29
Smc3	275	29	30
Rad21l	241	25	50

B

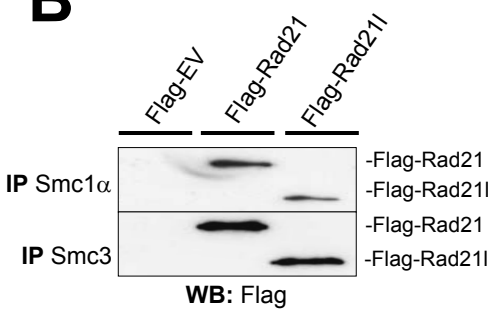

C

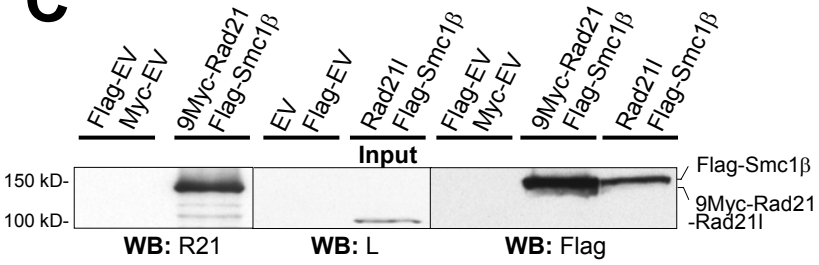

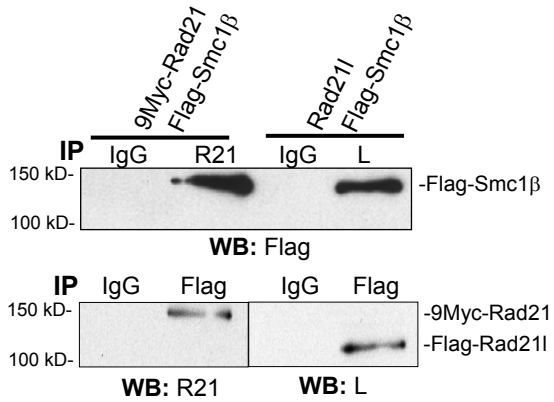

D

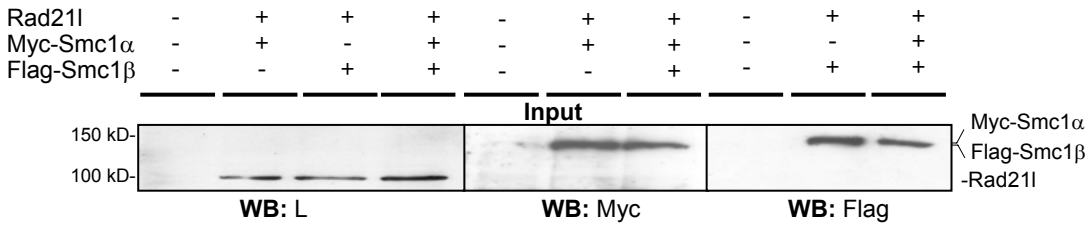

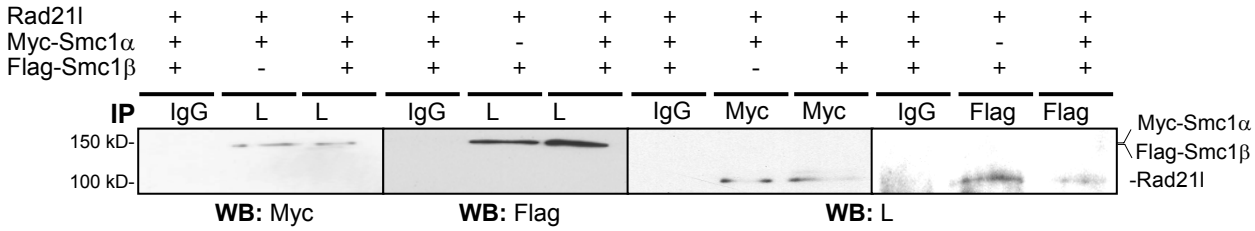

E

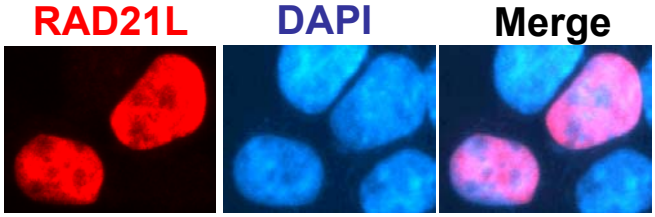

F

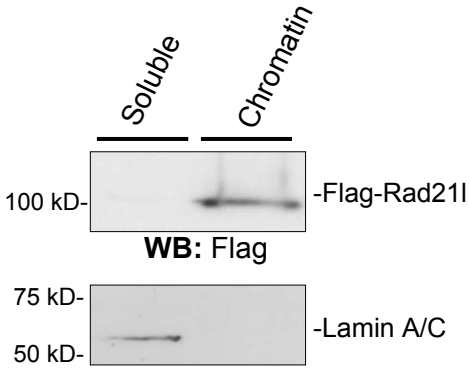

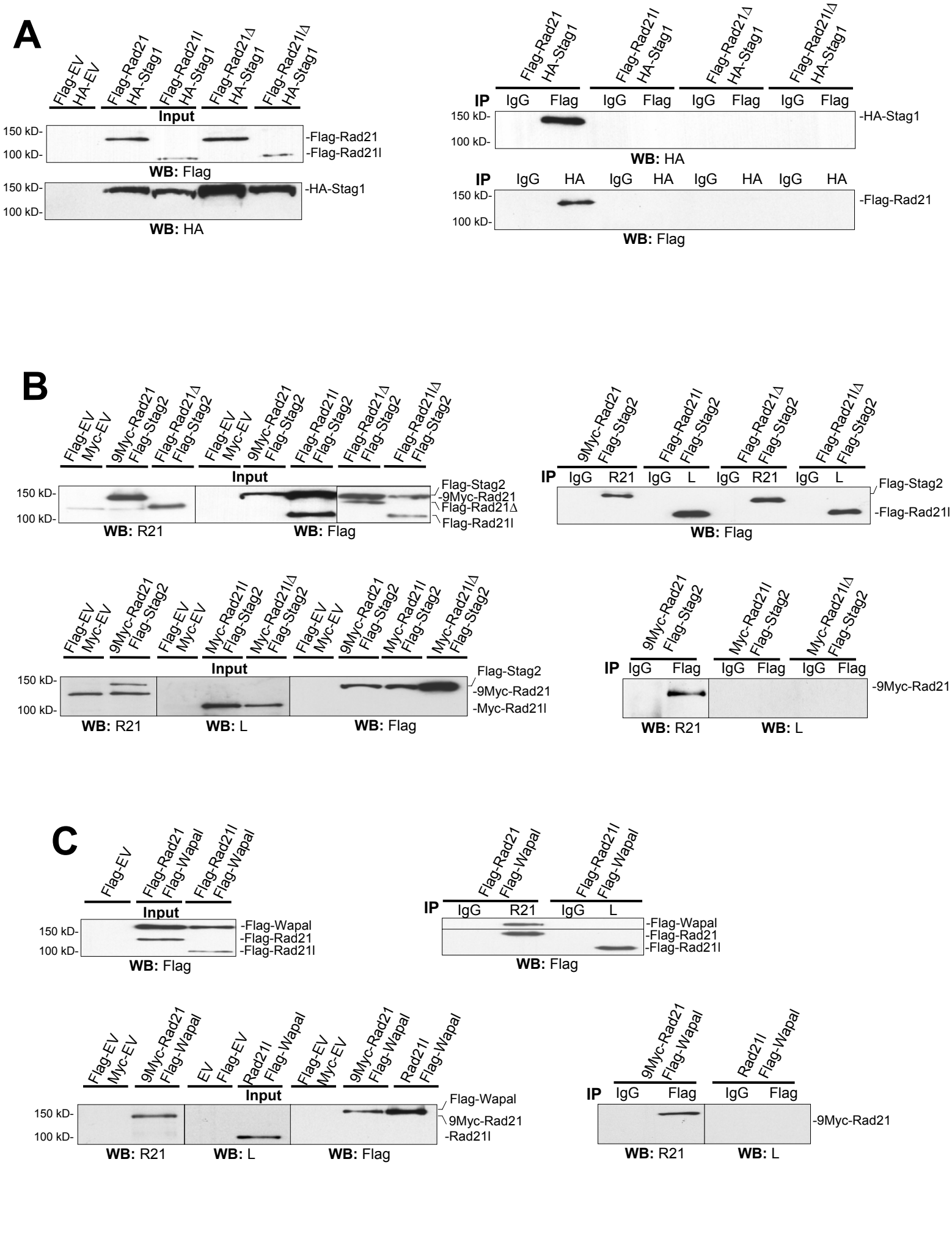
A
Flag-EV
HA-EV
Flag-Rad21
HA-Stag1
Flag-Rad21I
HA-Stag1
Flag-Rad21Δ
HA-Stag1
Flag-Rad21IΔ
HA-Stag1
Input
150 kD-
100 kD-
-Flag-Rad21
-Flag-Rad21I
WB: Flag
-HA-Stag1
WB: HA
IP
IgG
Flag
HA
-HA-Stag1
WB: HA
-Flag-Rad21
WB: Flag
B
Flag-EV
Myc-EV
9Myc-Rad21
Flag-Stag2
Flag-Rad21Δ
Flag-Stag2
Flag-Rad21I
Flag-Stag2
Flag-Rad21IΔ
Flag-Stag2
Input
Flag-Stag2
-9Myc-Rad21
Flag-Rad21Δ
Flag-Rad21I
WB: R21
WB: Flag
IP
IgG
R21
L
-Flag-Stag2
-Flag-Rad21I
WB: Flag
Myc-Rad21I
Flag-Stag2
Myc-Rad21IΔ
Flag-Stag2
-Myc-Rad21I
WB: L
-9Myc-Rad21
WB: R21
C
Flag-EV
Flag-Rad21
Flag-Wapal
Flag-Rad21I
Flag-Wapal
-Flag-Wapal
-Flag-Rad21
-Flag-Rad21I
WB: Flag
EV
Rad21I
-9Myc-Rad21
-Rad21I

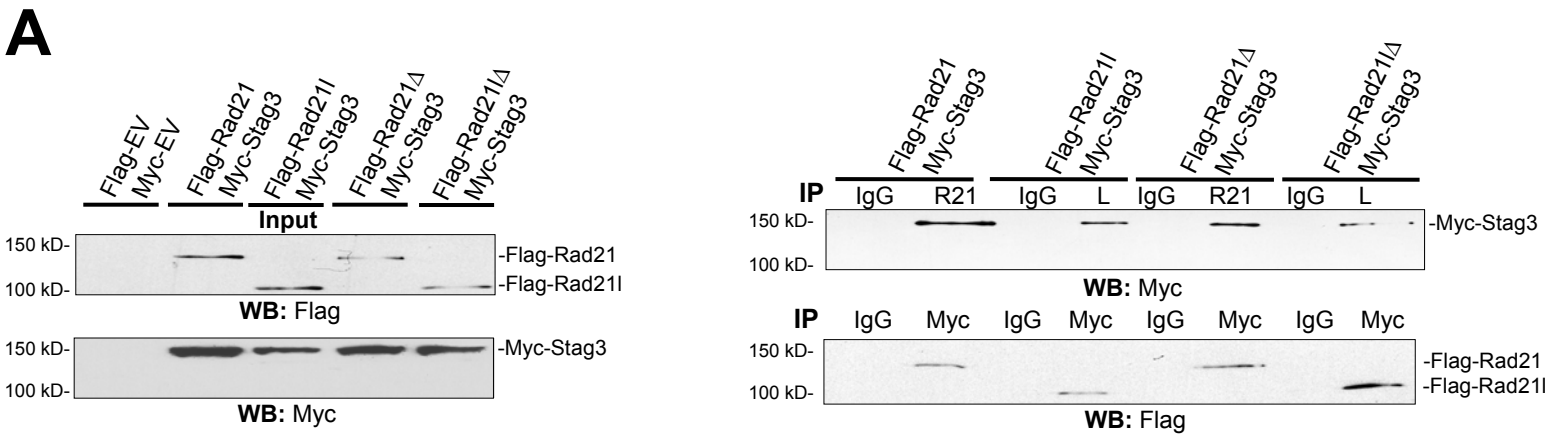
A
Flag-EV
Myc-EV
Flag-Rad21
Myc-Stag3
Flag-Rad21l
Myc-Stag3
Flag-Rad21Δ
Myc-Stag3
Flag-Rad21lΔ
Myc-Stag3
Input
150 kD-
100 kD-
-Flag-Rad21
-Flag-Rad21l
WB: Flag
150 kD-
100 kD-
-Myc-Stag3
WB: Myc
IP
IgG
R21
IgG
L
IgG
R21
IgG
L
150 kD-
100 kD-
-Myc-Stag3
WB: Myc
IP
IgG
Myc
IgG
Myc
IgG
Myc
IgG
Myc
150 kD-
100 kD-
-Flag-Rad21
-Flag-Rad21l
WB: Flag

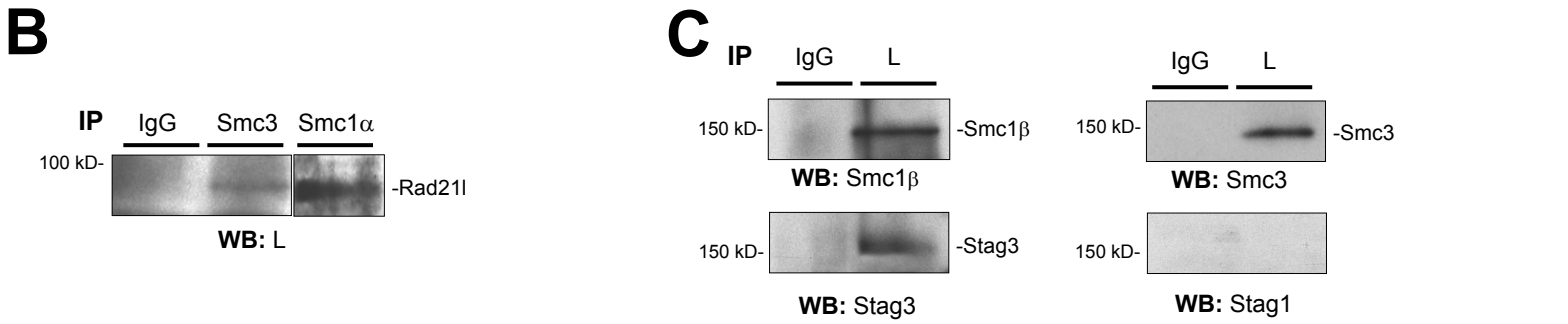
B
IP
IgG
Smc3
Smc1α
100 kD-
-Rad21l
WB: L
C
IP
IgG
L
150 kD-
-Smc1β
WB: Smc1β
150 kD-
-Stag3
WB: Stag3
IgG
L
150 kD-
-Smc3
WB: Smc3
150 kD-
WB: Stag1

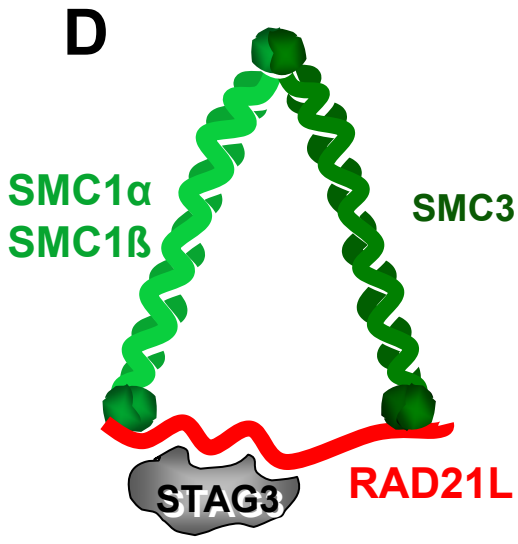
D
SMC1α
SMC1ß
SMC3
STAG3
RAD21L

A

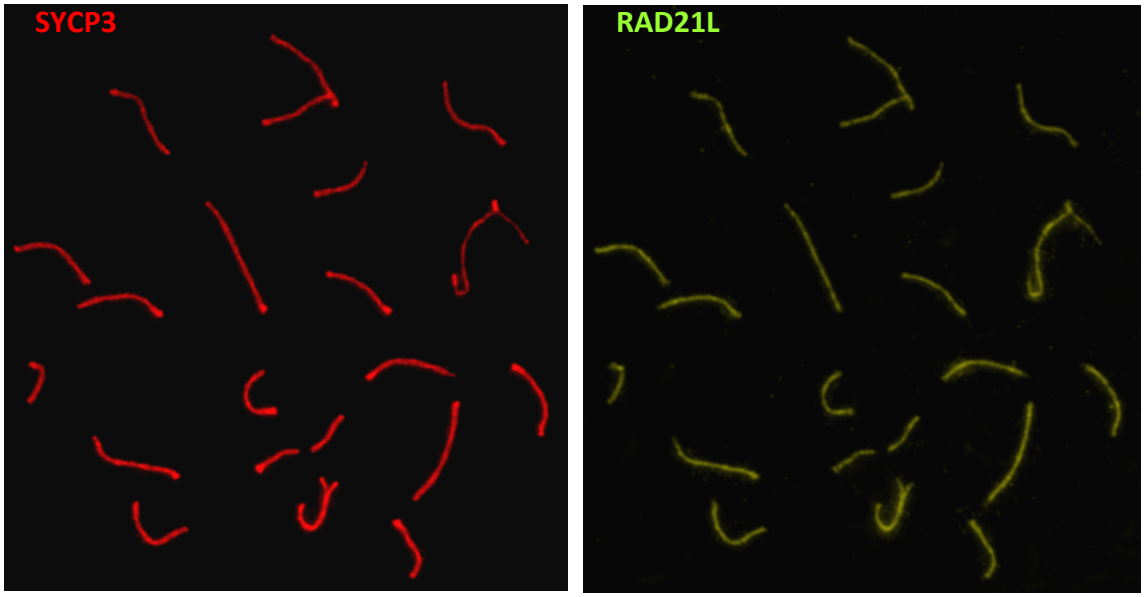

B

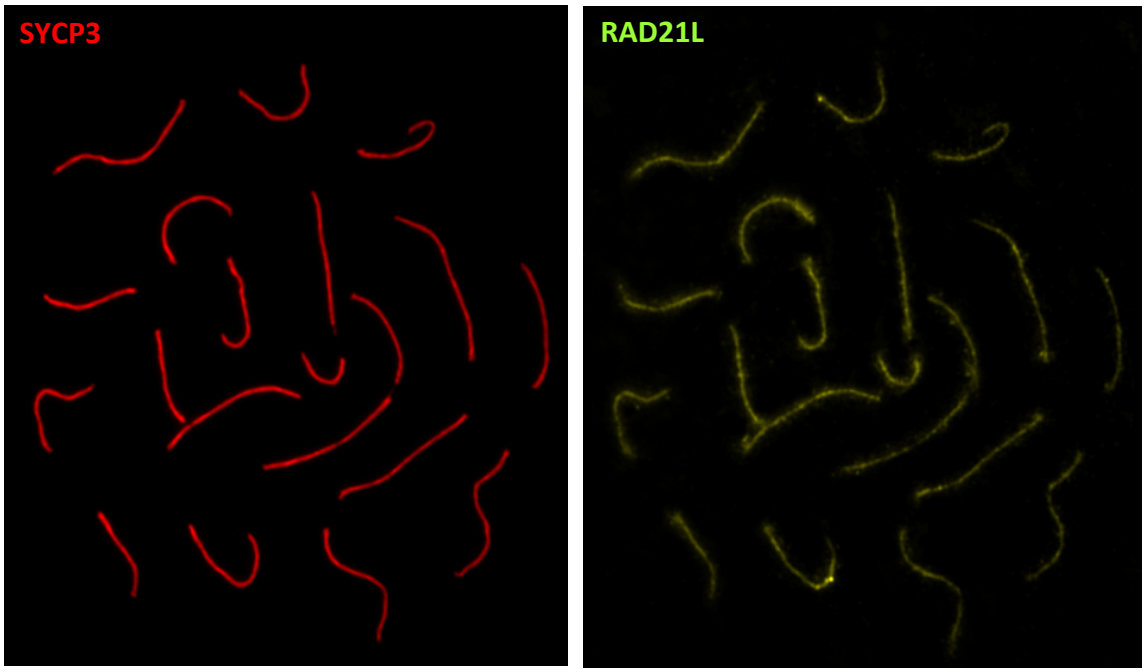

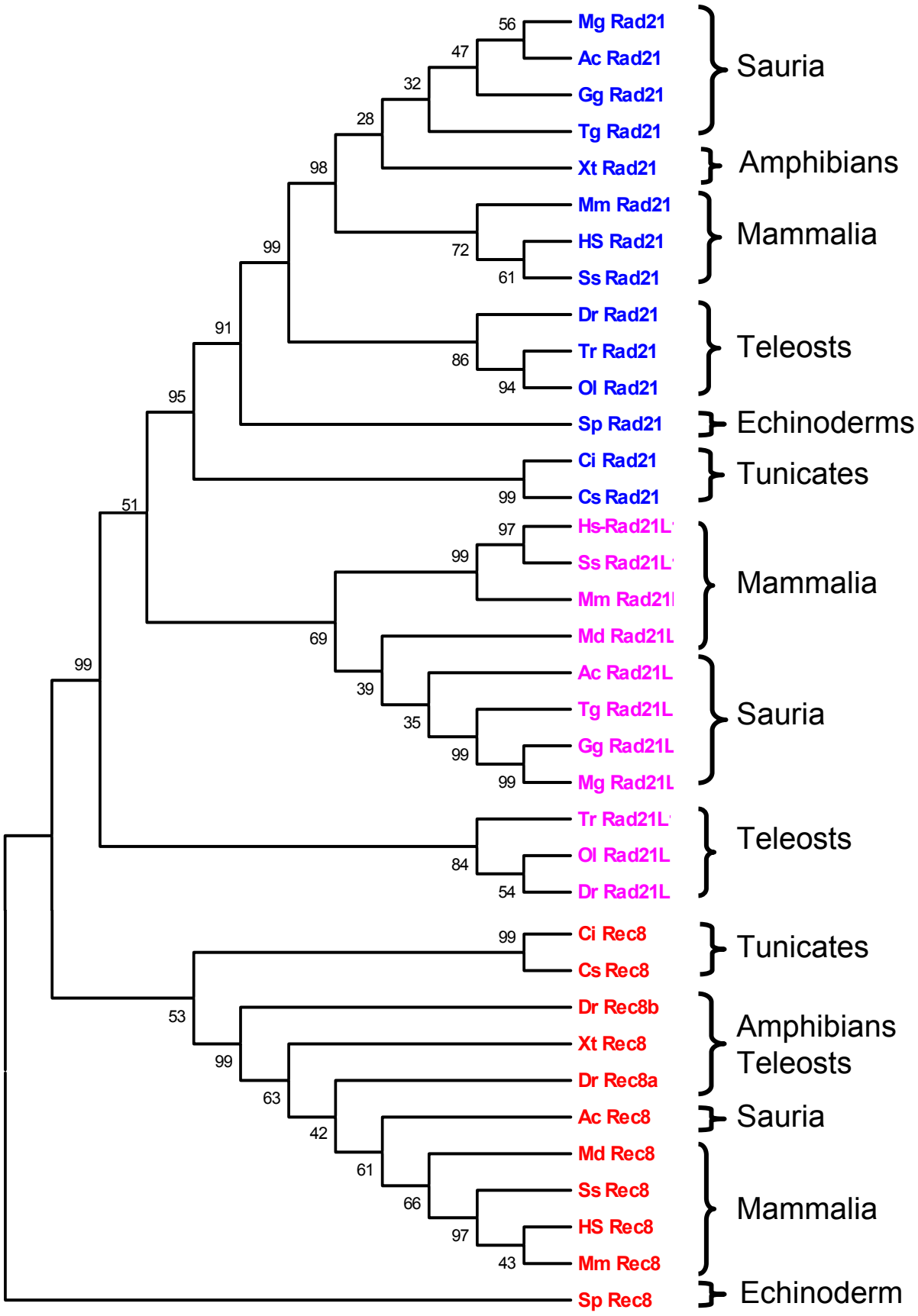
Mg Rad21
Ac Rad21
Gg Rad21
Tg Rad21
Xt Rad21
Mm Rad21
HS Rad21
Ss Rad21
Dr Rad21
Tr Rad21
Ol Rad21
Sp Rad21
Ci Rad21
Cs Rad21
Hs Rad21L
Ss Rad21L
Mm Rad21L
Md Rad21L
Ac Rad21L
Tg Rad21L
Gg Rad21L
Mg Rad21L
Tr Rad21L
Ol Rad21L
Dr Rad21L
Ci Rec8
Cs Rec8
Dr Rec8b
Xt Rec8
Dr Rec8a
Ac Rec8
Md Rec8
Ss Rec8
HS Rec8
Mm Rec8
Sp Rec8
Sauria
Amphibians
Mammalia
Teleosts
Echinoderms
Tunicates
Mammalia
Sauria
Teleosts
Tunicates
Amphibians
Teleosts
Sauria
Mammalia
Echinoderm